Applied Energy 219 (2018) 179–186

Contents lists available at ScienceDirect

Applied Energy

journal homepage: www.elsevier.com/locate/apenergy

Advancement of distributed energy methods by a novel high efficiency solar-assisted combined cooling, heating and power system

Na Zhang[a,*], Zefeng Wang[a,b], Noam Lior[c], Wei Han[a]

[a] Institute of Engineering Thermophysics, Chinese Academy of Sciences, Beijing 100190, China
[b] University of Chinese Academy of Sciences, Beijing, China
[c] Department of Mechanical Engineering and Applied Mechanics, University of Pennsylvania, Philadelphia, PA 19104-6315, USA

HIGHLIGHTS

- A solar assisted combined cooling, heating and power (SCCHP) system is proposed.
- Energy recovery improves matches between energy donors and receivers.
- Cascade utilization of input energies enables enhanced specific power generation.
- The fossil energy saving ratio of the proposed system reaches 30.4%.
- The exergy efficiency can be improved 6.18% compared with conventional trigeneration.

ARTICLE INFO

Keywords:
Distributed energy system
Combined cooling, heating and power system
Solar heat
Thermochemical upgrading
Fossil fuel saving

ABSTRACT

To improve the conversion efficiency of renewable energy use in high efficiency novel distributed energy systems, and the match between the energy donors and receivers in them, this paper proposes and analyzes a solar assisted combined cooling, heating and power system which supplies electricity, cooling and heat, with internal energy recovery and thermochemical upgrading, as their core component. The proposed system consists of a chemically recuperated gas turbine cycle, an absorption chiller and a heat exchanger, in which the reformer upgrades the absorbed turbine exhaust heat and solar heat into produced syngas chemical exergy, and rearranges the matches of energy donors and receivers both quantitatively and qualitatively. Based on well-established technologies including trigeneration, steam reforming and low/mid temperature solar heat collection, the system exhibits enhanced specific power generation and efficiency, and it commensurately reduces CO_2 emissions and saves depletable fossil fuel. The net solar-to-electricity efficiency is predicted to be 26–29% for a turbine inlet temperature of 980 °C. Compared with the stand-alone power, cooling and heating generation system, the reduction potential of fossil fuel consumption has been demonstrated to be 30.4% with a solar thermal share of 26%. Moreover, this system produces 33% less CO_2 emission than a conventional combined cooling, heating and power system with the same technology but without solar assistance. An excess electricity storage unit or storage of excess syngas can be considered to balance the difference between the supply and demand quantities.

1. Introduction

Distributed energy systems (DES), which are typically composed of a number of modular and small scale technologies and situated close to the end users, can be regarded as an essential complement to conventional centralized power network [1,2]. They have a number of advantages such as low transmission loss, low environmental emissions, and flexibility with multiple energy resources including fossil fuels, alternative fuels and renewable energy resources. In addition, they also have multiple energy production with cascade energy utilization, in the form of combined cooling, heating and power cogeneration (CCHP) systems [3–5], in which the heating and cooling demand is provided by using the residual heat from electricity generation, and thus achieve better performance in meeting customers' multi-energy demands and in energy saving with overall energy efficiency typically > 80%.

The research publications related to distributed energy systems mainly focus on system design, operation strategy and performance evaluation [6,7]. The CCHP system configuration used is mainly

* Corresponding author.
E-mail addresses: zhangna@iet.cn (N. Zhang), wangzefeng@iet.cn (Z. Wang), lior@seas.upenn.edu (N. Lior), hanwei@iet.cn (W. Han).

https://doi.org/10.1016/j.apenergy.2018.03.050
Received 7 November 2017; Received in revised form 12 March 2018; Accepted 18 March 2018

Nomenclature

A	energy level
CEM	specific CO_2 emission per kWh electricity generation [g/kWh]
COP	coefficient of performance
DNI	direct normal irradiation
E	exergy [kW]
LHV	lower heating value of fuel [kJ/kg]
m	mass flow rate [kg/s]
P	pressure [bar]
Q	heat [kW]
SR_f	fossil fuel saving ratio, Eq. (7)
T	temperature [°C]
TIT	turbine inlet temperature [°C]
W	power output [kW]
$X_{e,sol}$	solar exergy input share, Eq. (5)
X_{sol}	solar heat input share, Eq. (4)
η_b	gas boiler efficiency [%]
η_{col}	collector efficiency [%]
η_e	electrical generation efficiency, Eq. (2)
η_{ex}	system exergy efficiency, Eq. (3)
η_{sol}	solar-to-electricity efficiency [%], Eq. (6)
η_{th}	system thermal efficiency [%], Eq. (1)

Subscripts

c	cooling
col	collector
e	electrical
f	fuel
h	heating
net	net output
ref	reference system
rad	solar radiation
sep	separate generation system
sol	solar heat
0	environment state
1, 2… 18	states on the cycle flow sheet

determined by the available energy resources and energy conversion technologies [8–10]; and operation strategy by the variation of customers' energy demands. CCHP systems can theoretically be made very efficient and cost-effective by cascade utilization of the input energy. Practical systems, however, usually exhibit lower than expected energy efficiency, because the energy demand and supply are not in optimal match, and the distributed energy resources are thus not fully exploited. The application of appropriate operation strategy is an essential requirement to improve the off-design performance of CCHP systems [11–13].

Currently the design and optimization of distributed energy systems is mainly based on mathematical tools to integrate different types of energy resources and energy conversion technologies, with single or mixed targets with weighted combination of energy efficiency, annual energy consumption, annual cost, or CO_2 emission [14–16], usually resulting to a linear combination of available DES technologies and resources. The renewable energy resources, such as solar heat, are usually integrated at the low temperature end for complementary heat production with low energy conversion efficiency [17,18]. Increasing the share of renewable energy input in the energy system, on one hand brings more environmental benefits such as saving depletable fossil fuel and reducing pollutant emissions, but on the other hand lowers the system overall energy efficiency because renewable energy is generally associated with transience and low energy flux. Somma et al. [19] proposed an analysis that matches the quality levels of supply and demand by their exergy, by satisfying, if possible, low quality (exergy) thermal demands with low exergy sources such as solar thermal or waste heat, and electricity demands with high exergy sources, but it is still by direct use of solar thermal or power-generation waste heat. Different from the above mentioned method, solar heat can be upgraded to chemical energy of solar thermochemical fuels through some solar thermochemical processes and solar energy can thus be stored in the form of fuel for continuous use [20–22].

In this paper, the authors proposed and analyzed a solar assisted

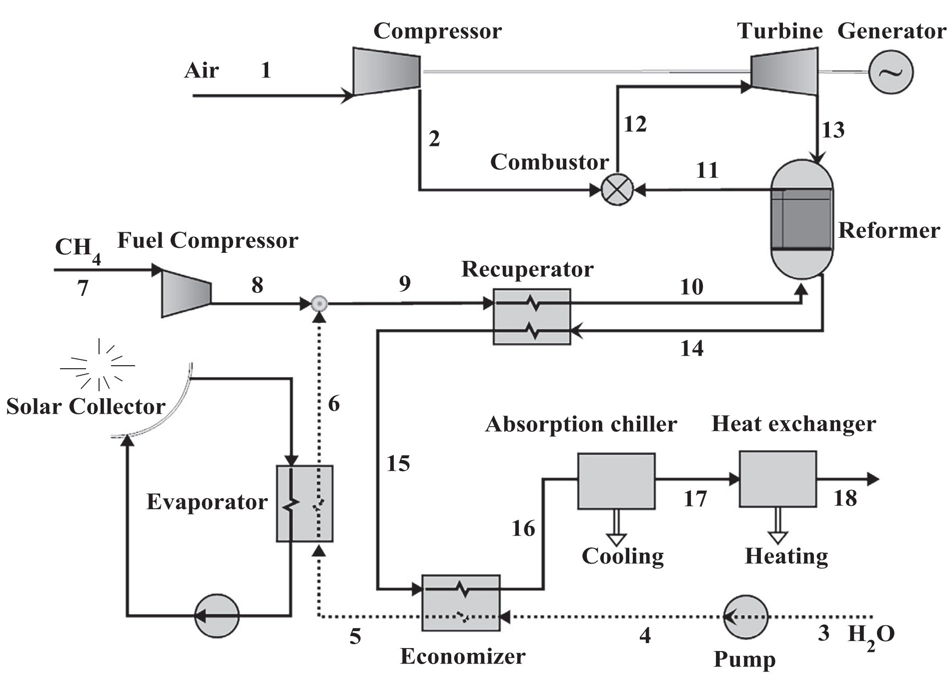

Fig. 1. Schematic diagram of the SCCHP system with solar heat integration.

combined cooling, heating and power (SCCHP) system. The involved energy recovery/regeneration enables cascade utilization of heat addition at different temperature levels, and thus balances the difference between energy demand and supply. Especially, turbine exhaust heat and solar heat are used indirectly for power generation, following their upgrading to syngas chemical exergy by a thermochemical conversion process. Exergy and energy analyses at design condition have been performed to reveal the energy saving process, showing that the same rates of electricity, heat and cooling outputs as those generated by their production using a separate system for each are attained by the proposed novel integrated system but with about 30% lower fuel input.

The system configuration is described in Section 2. Section 3 presents the main simulation assumptions and introduces the performance criteria composing the energy and exergy analysis. The design performance of the SCCHP system compared with the conventional CCHP system is discussed in Section 4. Moreover, the technical considerations for engineering application are presented. Finally, the paper is concluded in Section 5.

2. System configuration description

The proposed SCCHP system, which involves thermochemical upgrading of absorbed solar heat and turbine exhaust heat, is shown in Fig. 1. The system consists of a solar heat improved chemically recuperated gas turbine cycle (CRGT) for power generation [23,24], a gas turbine exhaust-heat driven absorption chiller, and a heat exchanger for heating production, respectively.

In this system, the water used for reforming (3) is preheated and then evaporated by solar heat to produce saturated steam (6). After being heated in the recuperator, the mixture of steam and natural gas enters the reformer to produce hydrogen-rich syngas (11), which is burned for the power-generating gas turbine. The turbine exhaust heat is recovered and utilized in a thermal cascade, by the reformer, economizer for water preheating, absorption chiller for cooling production and heat exchanger for heat production, in that order, from high to low temperature.

The steam reforming process is described by the following reactions [23]:

$$CH_4 + H_2O \leftrightarrow CO + 3H_2 \qquad \Delta H = 206.11\ \text{kJ/mol}$$

$$CO + H_2O \leftrightarrow CO_2 + H_2 \qquad \Delta H = -41.17\ \text{kJ/mol}$$

The first one is highly endothermic, the second, “shift reaction”, is exothermic. The thermo-chemical process has much higher heat recuperation capacity than the conventional thermal recuperation alone, and methane conversion increases with higher steam/fuel molar ratio, higher temperature, and lower pressure. The natural gas reforming process takes heat from both the turbine exhaust gas and the solar source, and adds the absorbed heat to the reforming products heating value, thereby increasing the power generation and efficiency beyond that with direct fossil fuel combustion alone.

The system employs a double effect LiBr-H_2O absorption chiller for cooling production at 5 °C for domestic building use. It consists of high-pressure (HP) and low-pressure (LP) generators, condenser, evaporator and absorber, solution pump, higher-temperature (HT) and lower-temperature (LT) heat exchangers, and throttling valves, as shown in Fig. 2. Taking advantage of the large boiling point difference between the refrigerant and the absorbent, the loops of refrigerant (1a-2a-3a/4a-5a-6a-7a) and of solution (8a-9a-10a-11a-12a-13a-14a-15a-16a-17a) are formed. Driven by the gas turbine flue gas heat in the high-pressure generator, it generates cooling by drawing lower-temperature heat Q_c in the evaporator. The off-design performance of the LiBr absorption chiller was investigated in [25]. It was found that as the gas turbine load drops from 100%, the *COP* of the absorption chiller first increases, from 1.3 at the full load operation to 1.31 at the gas turbine load of 65%, and then drops to 1.25 at the load of 25%. Since its variation is thus generally mild, the *COP* of the absorption chiller is in this paper taken to be 1.2.

3. System evaluation

3.1. Basic assumptions

This solar assisted combined cooling, heating and power (SCCHP) system is developed and simulated by application of the simulation software Aspen Plus [26]. The RK-Soave method is selected to estimate the thermodynamic data and phase behavior of the materials’ streams. The most relevant assumptions are summarized in Table 1.

The reformer model in this system is a built-in Gibbs Reactor available in Aspen Plus, and is applied for the calculation of chemical and phase equilibrium based on minimizing Gibbs free energy. The

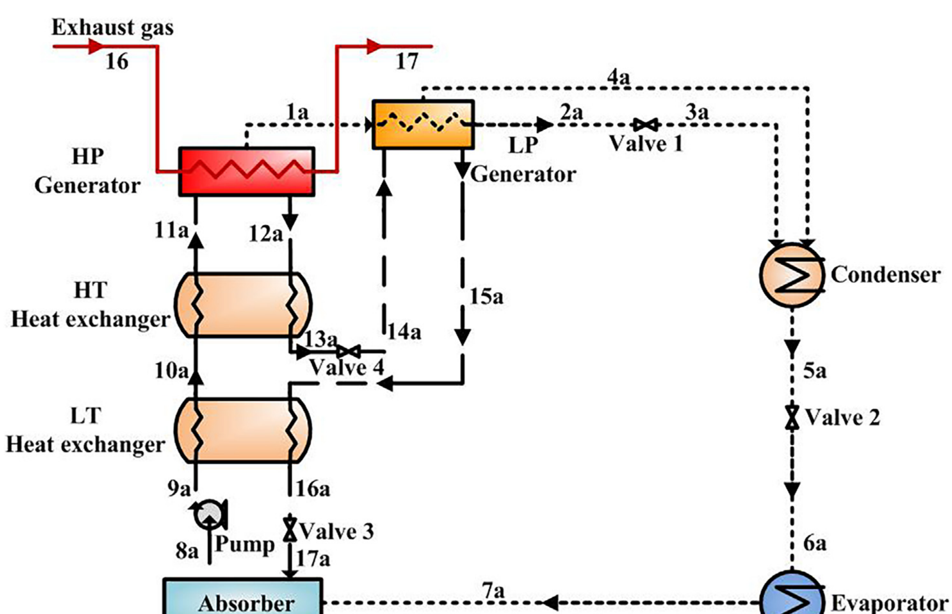

Fig. 2. A double-effect LiBr-H_2O absorption chiller.

Table 1
Main assumptions for the calculation.

			Source
Compressor	Pressure ratio	6.7	OPRA [27]
	Isentropic efficiency [%]	83	
	Inlet air mass flow rate [kg/s]	8.15	OPRA [27]
Turbine	Inlet temperature [°C]	980	OPRA [27]
	Isentropic efficiency [%]	88	
Combustor	Efficiency [%]	100	
	Pressure drop [%]	2	
Fuel compressor	Isentropic efficiency	80	
Reformer	Outlet pressure [bar]	6.79	
	Hot side pressure drop [%]	2	Kesser et al. [23]
	Code side pressure drop [%]	10	Kesser et al. [23]
	Minimum temperature difference [°C]	20	Kesser et al. [23]
	Reforming temperature [°C]	577.5	
Recuperator	Minimal temperature difference[°C]	20	
	Hot side pressure drop [%]	1	
	Cold side pressure drop [%]	2	
Economizer	Minimal temperature difference [°C]	15	
	Hot side pressure drop [%]	1	Kesser et al. [23]
	Code side pressure drop [%]	2	Kesser et al. [23]
Evaporator	Pressure drop [%]	4	
Pump	Efficiency [%]	80	
Absorption chiller	Coefficient of performance	1.2	Somma et al. [19]
	Outlet gas temperature [°C]	170	Somma et al. [19]
Heat exchanger	Efficiency [%]	98	
	Outlet stack temperature [°C]	130	Somma et al. [19]
Solar collector	Solar energy temperature [°C]	170	
	Solar collector efficiency [%]	76	
	Heat transfer efficiency [%]	95	
System	Mech. Efficiency × generator efficiency [%]	98	

degree of nonequilibrium in the reformer is represented by ΔT_{eq}, modeled by the chemical approach described in [23,24]. The calculated syngas temperature at the reformer exit is thus (T-ΔT_{eq}), and the syngas composition is the corresponding equilibrium one. The gas turbine was selected to be the OP16 micro gas turbine from OPRA company in the Netherlands [27], and the gas turbine model is validated by comparing the simulation results with the data from this manufacturer. Table 2 shows that the simulation results agree well with the manufacturer's data, with a relative error within 1% for the gas turbine exhaust temperature, power generation and efficiency. The relative error for gas mass flow rate is 4.5%, which perhaps is because of the different composition of the fuel, with pure methane used in our simulation. Validation of the basic CRGT cycle can be found in [28,29].

3.2. Performance criteria

The thermal efficiency of the system is defined as:

$$\eta_{th} = \frac{W_{net} + Q_h + Q_c}{Q_f + Q_{sol}} = \frac{W_{net} + Q_h + Q_c}{m_f \cdot LHV + Q_{sol}} \tag{1}$$

where W_{net}, Q_h and Q_c are the net electric power, heating and cooling outputs produced by the system, and $Q_f = m_f LHV$ is the fuel low heating value input, Q_{sol} is the solar heat input for steam generation.

For comparison with the simple gas turbine cycle, the electricity generation efficiency is defined as:

$$\eta_e = \frac{W_{net}}{Q_f + Q_{sol}} = \frac{W_{net}}{m_f \cdot LHV + Q_{sol}} \tag{2}$$

Because the system has multiple energy inputs and outputs with different energy qualities, the equivalent system exergy efficiency is defined to evaluate the performance of the SCCHP system. The methane exergy is assumed approximately to be 1.04 LHV; and the exergy of the solar heat supplied to the evaporator at a temperature of T_{sol} is calculated as the maximal work availability between T_{sol} and the ambient temperature T_0, i.e., that is $Q_{sol}(1-T_0/T_{sol})$. This exergy efficiency is thus given by:

$$\eta_{ex} = \frac{W_{net} + E_h + E_c}{E_f + E_{sol}} = \frac{W_{net} + E_h + E_c}{E_f + Q_{sol}(1-T_0/T_{sol})} \tag{3}$$

It is noteworthy that the exergy of the solar heat supply, and therefore also the value of η_{ex}, depend on the definition of the solar temperature T_{sol}, which is chosen here to be that of the solar heat at the temperature of its supply to the evaporator.

The contribution of the mid/low-temperature level solar heat can be measured by its share in the system total energy input:

$$X_{sol} = \frac{Q_{sol}}{Q_f + Q_{sol}} = \frac{Q_{sol}}{m_f \cdot LHV + Q_{sol}} \tag{4}$$

$$X_{e,sol} = \frac{Q_{sol}(1-T_0/T_{sol})}{E_f + Q_{sol}(1-T_0/T_{sol})} \tag{5}$$

To indicate the relative electricity generation performance of the solar heat contribution in the proposed SCCHP system, the net solar-to-electricity efficiency [29,30], η_{sol}, is defined as:

$$\eta_{sol} = \frac{W_{net}-W_{ref}}{Q_{rad}} = \frac{W_{net}-Q_f\,\eta_{e,ref}}{Q_{rad}} \tag{6}$$

in which W_{ref} is the power output produced by a reference system, here chosen to be the simple gas turbine cycle with the same methane input, $W_{ref} = Q_f \cdot \eta_{e,ref}$, Q_{rad} is the total solar energy incident on the solar concentrator, $Q_{rad} = Q_{sol}/(\eta_{col} \cdot \eta_{tr})$, and where η_{col} is the concentrating solar collector efficiency, and η_{tr} is the heat transfer efficiency from the collector to the cycle working fluid (in the Evaporator loop of Fig. 1).

The fossil fuel savings in comparison with a conventional system that generates the same amount of electricity, heating and cooling by separate units, is defined as the fossil fuel saving ratio:

$$SR_f = \frac{Q_{f,sep}-Q_f}{Q_{f,sep}} \tag{7}$$

where the heat input for the system using separate units is

$$Q_{f,sep} = (W_{net} + Q_c/COP_e)/\eta_{e,grid} + Q_h/\eta_b \tag{8}$$

The reference separate generation system is a typical commercial one, assumed to buy electricity from a grid with an average generation efficiency $\eta_{e,grid} = 35\%$, has an air source chiller driven by electricity with a COP_e of 4.5, and a natural gas boiler with an efficiency $\eta_b = 90\%$ [19,31].

The specific CO_2 emission per kWh electricity generation is defined

Table 2
Validation of the OP16 model.

Items	Data from the manufacturer	Simulation	Relative error %
Exhaust temperature (°C)	573	576.6	0.63
Exhaust gas mass flow (kg/s)	8.7	8.3	4.5
Electric power (kW)	1854	1867	0.7
Electrical efficiency (%)	26.9	27.0	0.37

as:

$$CEM = \frac{m_{CO_2} \times 3.6 \times 10^6}{W_{net}} \quad (9)$$

where *CEM* is the specific CO_2 emission (g/kWh), m_{co2} is the CO_2 mass emission rate in the turbine exhaust gas (kg/s).

4. Results and discussions

4.1. System performance

The proposed SCCHP system shown in Fig. 1 is simulated based on a steam/air ratio of 15%. Table 3 summarizes the thermodynamic parameters at key state points. When the steam/air ratio drops to zero, the system degrades to a conventional CCHP system without solar assistance; it is simulated with the same assumptions shown in Table 1.

The regular CCHP system is based on the same technologies as the SCCHP system except for the solar heat integration. It consists of an OP16 gas turbine, and the turbine exhaust heat is used to drive an absorption chiller and a heat recovery boiler for cooling and heating production, respectively. The comparison in Table 4 is based on the same turbine inlet temperature *TIT* of 980 °C, compressor pressure ratio of 6.7 and compressor inlet air mass flow rate of 8.15 kg/s. Because of the addition of solar heat generated steam in the SCCHP system, it demands different energy input amounts to maintain the same *TIT*, thus leads to different energy outputs than the regular CCHP system.

In the SCCHP system, solar heat at the temperature of 170 °C contributes 26.9% of the total heat input via water evaporation (for the reformer). The H_2O/C molar ratio in the reforming process is 8.5, which enables a conversion ratio of 64.8% of CH_4 at a temperature of 577.5 °C and pressure of 6.8 bar. Because of the increase of the working fluid by the generated vapor, the gas turbine generates 864.9 kW (46.3%) more electricity than the simple CCHP system. At the same time, since the higher temperature turbine exhaust heat is used as the reforming process heat, less exhaust heat is available for cooling production, which is therefore reduced by nearly 49% (2200 kW) from that of the simple CCHP system. The SCCHP system produces more electricity which has high energy quality than heat and cooling, and exhibits higher electricity generation efficiency and system exergy efficiency, but a much lower system thermal efficiency of 58.9% as compared with 97% of the conventional CCHP system.

It is noteworthy that the solar-to-electricity efficiency (η_{sol}) of SCCHP reaches 26% with a temperature of 170 °C, which is about the same as that of the simple gas turbine cycle (27% in Table 2), indicating that the system upgrades the mid-temperature solar heat and accomplishes its high-efficiency to power output. As compared with the separate production of power, heat and cooling, the fossil fuel saving ratio reaches 30.4% in the SCCHP system, which is also much higher than that of 19.3% in the conventional CCHP system without solar input. Corresponding to the fossil fuel saving, the specific CO_2 emission per kWh electricity generation is reduced in the SCCHP by 33%. If needed, any excess generated electricity can be stored and easily converted into cooling output by a mechanical compression chiller.

Fig. 3 shows the cascade recuperation of turbine exhaust heat. Of totally 5466 kW heat recuperation, about 26% at the high temperature end is used as reforming driving heat, another 30.8% is used to preheat the reactants (17% in the recuperator and 13.8% in the economizer). Most of the energy used in buildings is required to maintain indoor temperatures at around 20 °C to 26 °C, or to heat water at a temperature around 60 °C [19], they are commonly supplied by electricity or fossil fuels in the separate generation systems [32]. The required temperatures for space heating and cooling are low, and so is thus the quality of these energy demands. In the SCCHP system, only the lower temperature heat is used for cooling production (35%) and heat production (8.1%). Because the mid/low-temperature solar heat is used for water evaporation, the turbine exhaust heat only heats sensible heat sinks with varying temperature. The cascade utilization of exhaust turbine heat together with solar heat integration at different temperature levels facilitates the matching of quality levels of energy supply and demand, and thus avoids the waste of high-quality energy resources.

4.2. Exergy analysis

The SCCHP system has inputs from multiple energy resources, and produces multiple energy output type. An exergy analysis is therefore conducted to properly quantify different forms of energy inputs and outputs, and to locate exergy destructions and losses, and the results are summarized in Table 5. It is assumed that the SCCHP system supplies electricity, heat and cooling to a building, and the latter two are in the form of hot water at 60 °C (T_h) and the cooling at 5 °C (T_c).

The heat and cooling exergies are calculated by:

$$E_h = Q_h \cdot (1 - T_0/T_h) \quad (10)$$

$$E_c = Q_c \cdot (T_0/T_c - 1) \quad (11)$$

With 10.3% of its input exergy from solar heat at 170 °C, SCCHP converts 34.7% of the total exergy input into power generation. The relatively low temperatures of heat and cooling supply lead, as expected, to their low exergy outputs, 2.1% for cooling and 0.59% for heat output, respectively.

Fig. 4 presents the exergy loss in each component and the comparison with the conventional CCHP cycle without solar assistance. The highest exergy destruction is in the combustor where the fossil fuel chemical exergy degrades into thermal exergy. It is notable that the combustion exergy loss in the SCCHP cycle, of 33.5%, is even 3%-points lower than that in the conventional CCHP cycle, considering that the SCCHP cycle has a higher working fluid mass flow rate due to the 15% steam addition. Because combustion produces thermal heat at the same temperature of 980 °C in both systems, the combustion exergy loss difference therefore comes from the fuel side, syngas in the SCCHP system, and methane direct combustion in the conventional CCHP system. Based on the definition of 'energy level' as the ratio of exergy change to energy change [33]: $A = \Delta E/\Delta H$. Syngas has an energy level of about 0.96 (depending on its composition) [28,29], lower than that of methane for which it is 1.04. The reformer can therefore be considered as an energy level lever: driven by the drop of the energy level from methane to syngas, it lifts the energy level of the absorbed solar heat and turbine exhaust heat into syngas chemical exergy.

Another significant exergy loss reduction appears in the absorption

Table 3
Main stream states of the SCCHP system.

No.	T	P	m	Molar composition (%)						
	[°C]	[bar]	[kg/s]	CH_4	H_2	CO	CO_2	H_2O	O_2	N_2
1	25	1.013	8.15						21	79
2	279.6	6.79	8.15						21	79
3	25	2	1.222					100		
4	25	8.18	1.222					100		
5	170.5	8.02	1.222					100		
6	168.8	7.7	1.222					100		
7	25	5	0.136	100						
8	68.6	7.7	0.136	100						
9	164.6	7.7	1.358	11.1				88.9		
10	461.2	7.54	1.358	11.1				88.9		
11	577.5	6.79	1.358	3.4	24.4	0.7	5.6	65.9		
12	980	6.65	9.508				2.4	23.6	11.8	62.2
13	597.5	1.06	9.508				2.4	23.6	11.8	62.2
14	481.2	1.04	9.508				2.4	23.6	11.8	62.2
15	402.5	1.03	9.508				2.4	23.6	11.8	62.2
16	338.2	1.03	9.508				2.4	23.6	11.8	62.2
17	170	1.02	9.508				2.4	23.6	11.8	62.2
18	130	1.01	9.508				2.4	23.6	11.8	62.2

Table 4
Performance comparison between the SCCHP and CCHP systems.

	SCCHP	CCHP
Turbine inlet temperature [°C]	980	980
Compressor pressure ratio	6.7	6.7
Compressor inlet air mass flow rate [kg/s]	8.15	8.15
Steam/air ratio	0.15	0
Energy input		
Fuel LHV Q_f [kW]	6784.55	6916.98
Solar heat input [kW]	2498.98	0
Energy output		
Power output W_{net} [kW]	2732.14	1867.28
Heating Q_e [kW]	444.94	351.40
Cooling Q_c [kW]	2295.78	4496.23
Solar thermal share X_{sol} [%]	26.92	0
Solar exergy share E_{sol} [%]	10.33	0
System thermal efficiency η_{th} [%]	58.86	96.98
Electrical generation efficiency η_e [%]	29.43	27.0
System exergy efficiency η_{ex} [%]	37.40	31.22
Solar-to-electricity efficiency η_{sol} [%]	26.02	
Energy saving ratio SR_f [%]	30.40	19.31
Specific CO_2 emission [g/kWh]	490.2	731.2

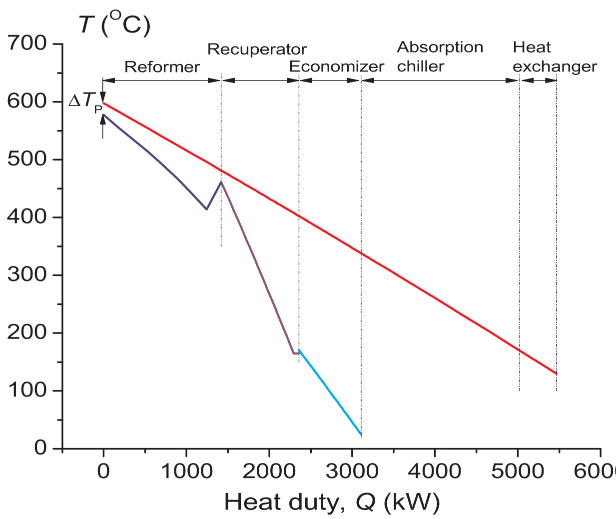

Fig. 3. Turbine exhaust heat recuperation process in the SCCHP system.

Table 5
Exergy analysis result of the SCCHP cycle.

	[MW]	[% of the total exergy input]
EXERGY INPUTS		
Fuel	7057.4	89.7
Solar heat	813.2	10.3
EXERGY OUTPUT		
Power generation	2732.1	34.7
Cooling	165.1	2.10
Heat	46.7	0.59
EXERGY LOSSES		
Combustor	2634.2	33.5
Reformer	99.0	1.26
Recuperator	182.3	2.32
Compressor	203.2	2.58
Turbine	237.9	3.02
Absorption chiller	658.1	8.36
Heat exchanger	99.3	1.26
Economizer	262.7	3.34
Water pump & fuel compressor	3.64	0.05
Flue gas	490.6	6.23
Mechanical loss	55.8	0.71

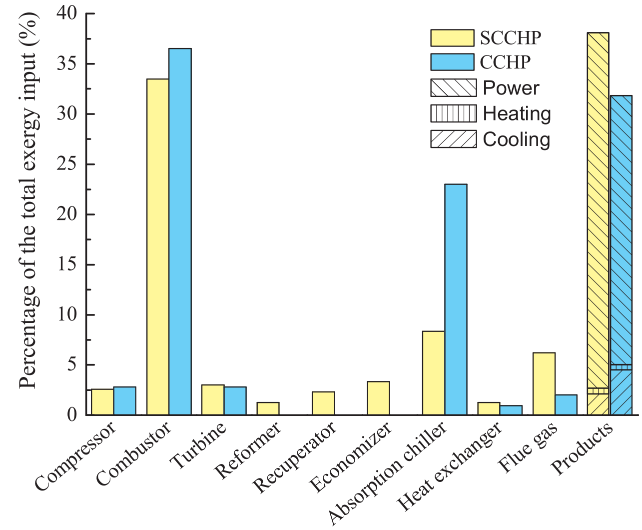

Fig. 4. Exergy destruction in main components and system products.

chiller, from 23% in the conventional CCHP system to 8.3% in the SCCHP system. In the conventional CCHP system, the turbine exhaust heat at the temperature of 576 °C is used to produce cooling at 5 °C. In the SCCHP system, the higher temperature turbine exhaust heat is recovered in the reformer for syngas production, and further to electricity generation. Only the lower end of the turbine exhaust heat is employed for cooling and heating production. In this way, the low energy level demands are met by only low quality energy sources.

Because of the addition of steam, the SCCHP system exhibits higher flue gas exergy loss as compared with the conventional CCHP system; and the reformer and steam generation introduce additional exergy losses. The exergy loss in the reformer and recuperator are, however, relatively small thank to the good thermal match in these components.

The reformer serves as a conjunction of energy recovery and upgrading, it shifts energy between lower and higher quality zones to reduce the energy level mismatches in different components. As a result, compared with the conventional CCHP system, the SCCHP system produces 864 kW more high quality electricity, and 2.4 kW less cooling exergy.

4.3. Performance analysis in the typical day

The respective daily simulation results of the SCCHP system are discussed in this section. In this paper, the solar irradiation date in Beijing is used to present the performance of the proposed system at part-load conditions. The hourly *DNI* and X_{sol} of the typical summer day are presented in Fig. 5. From 7 am, solar energy is transformed into the chemical energy contained in the syngas by the chemically recuperated gas turbine cycle and the X_{sol} quickly reaches the highest value of 26.93% at 9 am. In this process, the available syngas cannot satisfy the production of the SCCHP system and the lack of part must be provided by the natural gas when the X_{sol} increases from 0 to 26.93%. From 9 am to 3 pm, the production of syngas is able to meet the fuel supply of the SCCHP system. The X_{sol} remains constant although the *DNI* has the peak value of 869 W/m^2 at 12 am. Similar to the above description, the natural gas supplements syngas as fuel input to the SCCHP system.

The SCCHP system for a five-star hotel of 88400 m^2 including office and guest rooms as the reference building is modeled [34]. The hourly electricity, cooling and heating demands of the reference building for a typical day is shown in Fig. 6. The SCCHP system is operated under the following electric load operation strategy, thus the electric demand is satisfied by the gas turbine. The lack of heat is provided by the auxiliary boiler when the surplus heat contained in flue gas cannot satisfy heat for cooling and hot- water production in the absorption chiller and heat

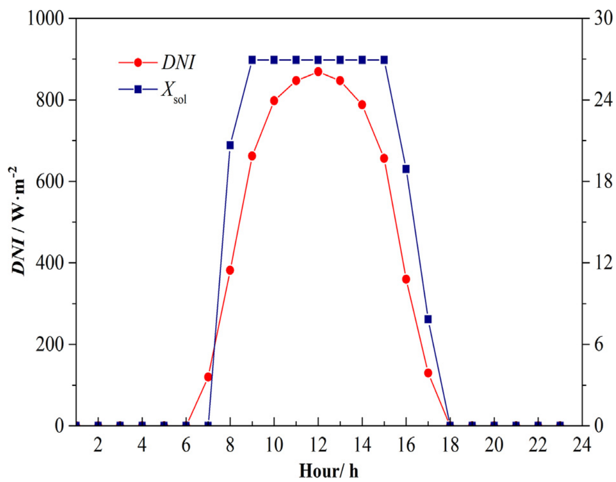

Fig. 5. *DNI* and solar thermal share on summer representative day.

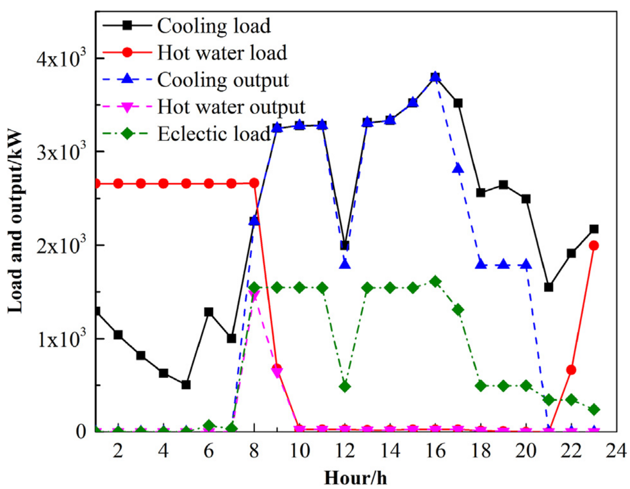

Fig. 6. Variations of building energy demand and energy output.

exchanger, respectively. We assume that the electric efficiency is a third- order polynomial that is connected to the part-load rate of the gas turbine. The *COP* of the absorption chiller is assumed as constant of 1.2. The thermal demand is satisfied by the auxiliary boiler from 9 pm to 7am because the gas turbine is turned off. The electric demand of the reference building increases sharply from 7am to 8am; and therefore the X_{sol} begins to increase from 7am despite the increase in *DNI* from 6am as shown in Fig. 5.

The solar energy complements fuel input from 7am to 6pm (11h), which effectively improves the energy-saving and environmental performance of the SCCHP system.

4.4. Technical considerations

As for the energy-saving and environmental friendly performance, the conventional CCHP system associated renewable energy has attracted continuing attention. In this paper, the function of energy recovery/regeneration was demonstrated by introducing and analyzing the novel SCCHP, a solar heat thermochemically-assisted CCHP system, in which mid/low-temperature solar heat is used to evaporate the reforming water, higher-temperature turbine exhaust heat provides the reforming process heat, and lower-temperature turbine exhaust heat is used for cooling and heat production, thus achieving cascade utilization of heat addition at different temperature levels.

Reforming drops the energy level of methane to that of syngas, leading to the reduction of combustion exergy destruction, and recovers the upper end of the turbine exhaust heat to avoid its mismatching with low energy quality demand, and converts it together with the mid/low-temperature solar heat into syngas chemical exergy, which is further efficiently converted into electricity in the gas turbine. The reformer rematches the energy donors and receivers both quantitatively and qualitatively, thereby leading to significant fossil fuel saving and CO_2 emission reduction in a magnitude that exceed the solar heat input ratio.

Due to the variation of the energy demands, and sometimes energy supply, the distributed energy system needs to run frequently under off-design conditions, at which gas turbine performance deteriorates. The SCCHP system relieves this problem by allowing adjustments of the ratio of turbine exhaust heat for heat and cooling, and the solar heat can also be used for cooling or heat production. The system is also amenable to storage of energy for balancing the quantity difference of energy supply and demand, and depending on the user's demand variation, different energy storage technologies can be considered: for example, if the cooling and heating production can't meet the user's demand, and electricity is over-generated, an electricity storage unit can then be implemented to allow the power section to run under design condition and store the excessive generated electricity, which can be converted into cooling or heating output efficiently as needed. Alternatively, excess syngas produced by the reformer can be diverted from the turbine for easy storage and use as needed. The off-design performance is an important issue and should be addressed separately.

The proposed system also offers significant alleviation of environmental problems associated with the generation of power, cooling and heating. It reduces the specific CO_2 emissions by 33% as compared to the conventional CCHP system and reduces the thermal NO_x formation in the combustion to < 1 ppm because of the presence of large quantity of steam in the syngas. Furthermore, with the saving of fossil fuel, the other pollutants are also reduced in the proposed system, which heightens the competitiveness with other polygeneration systems. The system retains its thermodynamic advantages of high-efficiency conversion of low temperature heat with energy sources other than solar heat, such as waste or geothermal heat, and its CO_2 emission reduction advantages when the heat sources do not involve CO_2 emission.

The technologies contained in the SCCHP system can be achieved and commercially available. The system uses a mid/low-temperature solar collector combined steam generator. The widely applied parabolic trough solar concentrating collectors [35] may be used to provide heat at ~170 °C for water evaporation.

5. Concluding remarks

A solar assisted combined cooling, heating and power system was proposed, which provides electricity, cooling and heat for distributed energy customers and for other users. The higher-temperature part of the turbine exhaust heat and the lower-temperature solar heat contribute to syngas production and are thereby converted to additional fuel heating value. Cascade utilization of different energy resources at different temperature levels has been established, and the improved energy level match in the system result in increased power generation and efficiency, and thereby significant fossil fuel saving and CO_2 emission reduction beyond the solar heat input ratio. Specifically, the net solar-to-electricity efficiency (η_{sol}), is predicted to be 26–29% with a turbine inlet temperature at 980 °C. Compared with a conventional system that generates the same amount of electricity, heating and cooling by separate units, a fossil energy saving ratio reaches 30.4% with a solar thermal share of 26%. Moreover, saving fossil fuel leads to a commensurate 33% reduction of CO_2 emission compared with the conventional trigeneration system with the same technology and without solar assistance.

An electricity storage unit can be employed to store the excessive electricity generation, it helps the gas turbine to run under design conditions and allow the stored electricity to cover the variable cooling and heating loads if and when needed. Alternatively, excess syngas produced by the reformer can be diverted from the turbine for easy storage and use as needed.

Acknowledgment

The authors gratefully acknowledge the support of the National Key Fundamental Research Project of China (No. 2014CB249202) and the National Natural Science Foundation of China (No. 51576191).

References

[1] Akorede MF, Hizam H, Pouresmaeil E. Distributed energy resources and benefits to the environment. Renew Sustain Energy Rev 2010;14(2):724–34.
[2] Zhou Z, Liu P, Li Z, Ni W. An engineering approach to the optimal design of distributed energy systems in China. Appl Therm Eng 2013;53(2):387–96.
[3] Cho H, Smith AD, Mago P. Combined cooling, heating and power: a review of performance improvement and optimization. Appl Energy 2014;136:168–85.
[4] Liu M, Shi Y, Fang F. Combined cooling, heating and power systems: a survey. Renew Sustain Energy Rev 2014;35:1–22.
[5] Borgogno R, Mauran S, Stitou D, Marck G. Thermal-hydraulic process for cooling, heating and power production with low-grade heat sources in residential sector. Energy Convers Manage 2017;135:148–59.
[6] Ju L, Tan Z, Li H, Tan Q, Yu X, Song X. Multi-objective operation optimization and evaluation model for CCHP and renewable energy based hybrid energy system driven by distributed energy resources in China. Energy 2016;111:322–40.
[7] Rahman HA, Majid MS, Jordehi AR, Kim GC, Hassan MY, Fadhl SO. Operation and control strategies of integrated distributed energy resources: a review. Renew Sustain Energy Rev 2015;51:1412–20.
[8] Ren H, Gao W. A MILP model for integrated plan and evaluation of distributed energy systems. Appl Energy 2010;87(3):1001–14.
[9] Jradi M, Riffat S. Tri-generation systems: energy policies, prime movers, cooling technologies, configurations and operation strategies. Renew Sustain Energy Rev 2014;32:396–415.
[10] Braslavsky JH, Wall JR, Reedman LJ. Optimal distributed energy resources and the cost of reduced greenhouse gas emissions in a large retail shopping centre. Appl Energy 2015;155:120–30.
[11] Kang L, Yang J, An Q, Deng S, Zhao J, Wang H, et al. Effects of load following operational strategy on CCHP system with an auxiliary ground source heat pump considering carbon tax and electricity feed in tariff. Appl Energy 2017;194:454–66.
[12] Song X, Liu L, Zhu T, Zhang T, Wu Z. Comparative analysis on operation strategies of CCHP system with cool thermal storage for a data center. Appl Therm Eng 2016;108:680–8.
[13] Fumo N, Mago PJ, Chamra LM. Emission operational strategy for combined cooling, heating, and power systems. Appl Energy 2009;86:2344–50.
[14] Mago P, Chamra L. Analysis and optimization of CCHP systems based on energy, economical, and environmental considerations. Energy Build 2009;41(10):1099–106.
[15] Ren H, Zhou W, Ki Nakagami, Gao W, Wu Q. Multi-objective optimization for the operation of distributed energy systems considering economic and environmental aspects. Appl Energy 2010;87(12):3642–51.
[16] Falke T, Krengel S, Meinerzhagen AK, Schnettler A. Multi-objective optimization and simulation model for the design of distributed energy systems. Appl Energy 2016;184:1508–16.
[17] Wang J, Yang Y, Mao T, Sui J, Jin H. Life cycle assessment (LCA) optimization of solar-assisted hybrid CCHP system. Appl Energy 2015;146:38–52.
[18] Chang H, Wan Z, Zheng Y, Chen X, Shu S, Tu Z, et al. Energy analysis of a hybrid PEMFC–solar energy residential micro-CCHP system combined with an organic Rankine cycle and vapor compression cycle. Energy Convers Manage 2017;142:374–84.
[19] Di Somma M, Yan B, Bianco N, Graditi G, Luh PB, Mongibello L, et al. Operation optimization of a distributed energy system considering energy costs and exergy efficiency. Energy Convers Manage 2015;103:739–51.
[20] Kong H, Hao Y, Wang H. A solar thermochemical fuel production system integrated with fossil fuel heat recuperation. Appl Therm Eng 2016;108:958–66.
[21] Pregger T, Graf D, Krewitt W, Sattler C, Roeb M, Möller S. Prospects of solar thermal hydrogen production processes. Int J Hydrogen Energy 2009;34:4256–42672.
[22] Su B, Han W, Jin H. Proposal and assessment of a novel integrated CCHP system with biogas steam reforming using solar energy. Appl Energy 2017;206:1–11.
[23] Kesser KF, Hoffman M, Baughn J. Analysis of a basic chemically recuperated gas turbine power plant. J Eng Gas Turbines Power 1994;116(2):277–84.
[24] Han W, Jin H, Zhang N, Zhang X. Cascade utilization of chemical energy of natural gas in an improved CRGT cycle. Energy 2007;32(4):306–13.
[25] Han W, Chen Q, Lin R, Jin H. Assessment of off-design performance of a small-scale combined cooling and power system using an alternative operating strategy for gas turbine. Appl Energy 2015;138:160–8.
[26] Aspen Plus. Aspen Technology, Inc., version 7.3. Available from: http://www.aspentech.com/.
[27] http://www.opra.nl/en/OPRA-WEB-Products-Products/Product-sheets/Product-sheets/;OPRA; 2014 [Technical specification sheets].
[28] Zhang N, Lior N. Use of low/mid-temperature solar heat for thermochemical upgrading of energy, part I: application to a novel chemically-recuperated gas-turbine power generation (SOLRGT) system. J Eng Gas Turbines Power 2012;134(7):072301.
[29] Zhang N, Lior N, Luo C. Use of low/mid-temperature solar heat for thermochemical upgrading of energy, part II: a novel zero-emissions design (ZE-SOLRGT) of the solar chemically-recuperated gas-turbine power generation system (SOLRGT) guided by its exergy analysis. J Eng Gas Turbines Power 2012;134(7):072302.
[30] Hong H, Jin H, Sui J, Ji J. Mechanism of upgrading low-grade solar thermal energy and experimental validation. J Sol Energy Eng 2008;130(2):021014.
[31] Barbosa Jr JR, Ribeiro GB, de Oliveira PA. A state-of-the-art review of compact vapor compression refrigeration systems and their applications. Heat Transf Eng 2012;33(4–5):356–74.
[32] Schmidt D. Low exergy systems for high-performance buildings and communities. Energy Build 2009;41(3):331–6.
[33] Jin H, Ishida M. Graphical exergy analysis of complex cycles. Energy 1993;18:615–25.
[34] Wang Z, Han W, Zhang N, Su B, Gan Z, Jin H. Effects of different alternative control methods for gas turbine on the off-design performance of a trigeneration system. Appl Energy 2018;215:227–36.
[35] Price H, Lupfert E, Kearney D, Zarza E, Cohen G, Gee R, et al. Advances in parabolic trough solar power technology. J Sol Energy Eng 2002;124(2):109–25.